

# PROGRESS OF APPLIED SUPERCONDUCTIVITY RESEARCH AT MATERIALS RESEARCH LABORATORIES, ITRI (TAIWAN)

R. S. Liu and C. M. Wang

Materials Research Laboratories, Industrial Technology Research Institute,  
Hsinchu, Taiwan, R.O.C.

## Abstract

A status report based on the applied high temperature superconductivity (HTS) research at Materials Research Laboratories (MRL), Industrial Technology Research Institute (ITRI) is given. The aim is to develop fabrication technologies for the high- $T_C$  materials appropriate to the industrial application requirements. To date, the majorities of works have been undertaken in the areas of new materials, wires/tapes with long length, prototypes of magnets, large-area thin films, SQUIDs and microwave applications.

## 1. Introduction

High temperature superconductivity (HTS) research at Materials Research Laboratories (MRL), Industrial Technology Research Institute (ITRI), was started from February 1987. The goals for the high- $T_C$  superconductivity research at MRL/ITRI are as follows :

- Search for new high- $T_C$  materials.
- Develop techniques for mass production of superconducting and homogeneous with small particle size powders .
- Establish long length and high- $J_C$  wire fabrication techniques.
- Fabrication of high- $T_C$  superconducting current lead and magnet.
- Establish high quality and large area superconducting thin film fabrication techniques.
- Thin film application researches in SQUIDs and microwave devices.

Therefore, the simplest target for the HTS research at the MRL/ITRI is to develop fabrication technologies for the high- $T_C$  materials appropriate to the industrial application requirements. To date, the majorities of works have been undertaken in the areas of new materials, wires/tapes with long length, prototypes of magnets, large-area thin films, SQUIDs and

microwave applications. The concept of the metal-superconductor-insulator transition has been applied to fine-tune the optimal  $T_c$ 's for new high- $T_c$  superconducting material systems. Superconductivity up to 135 K has been achieved in the Hg-containing cuprates. The process for producing a single pancake Bi-2223 coil which can generate a magnetic field of  $\sim 437$  Gauss at 77 K and self field has been set-up. High quality YBCO thin films ( $T_c \geq 88$  K and  $J_c \geq 10^6$  A/cm<sup>2</sup> at 77 K) with diameter around 2 inches have been made by laser ablation and hot-wall sputtering. SQUIDs and Microwave devices (such as resonator) have also been developed. This research is mainly supported by the Ministry of Economic Affairs (R.O.C.). In Table 1 we list the budget and manpower of the HTS research at the MRL/ITRI. Moreover, several local companies have joined the research program with the MRL/ITRI since 1988 indicating that the industry in Taiwan has perceived what a magnificent impact would be if HTS products are commercialized.

Table 1. The budget and manpower of the HTS research at the MRL/ITRI supported by the Ministry of Economic Affairs.

Fiscal Year (FY)	Budget (US\$ in million)	Manpower (person)
FY 90	2.650	28
FY 91	3.313	33
FY 92	2.630	33
FY 93	2.362	32
FY 94	1.637	23

Some of our recent achievements on the HTS research at the MRL/ITRI are summarized as the following sections.

## 2. The chemical control of high- $T_c$ superconductivity

The substitutional chemistry of a wide range of cuprate superconducting materials has been investigated at the MRL/ITRI with the general aims of optimising the critical temperature, current density, phase purity, chemical stability and ease of synthesis. Here, we demonstrate a typical example based on the chemical control of high- $T_c$  superconductivity through the metal-superconductor-insulator transition. Bulk superconductivity, up to 110 K, in the system  $(Tl_{0.5}A_{0.5})(Ca_{0.8}R_{0.2})Sr_2Cu_2O_7$  ( $A = Pb$  or  $Bi$ ;  $R = Y$  or rare earth elements) has been reported.<sup>1-4</sup> This septenary system has the highest  $T_c$  among the thallium cuprate systems with the so-called 1212 structure. The structure of the 1212 phase  $(Tl_{0.5}Pb_{0.5})Sr_2(Ca_{1-x}Y_x)Cu_2O_7$  can be described in terms of an intergrowth of double rock salt-type layers [ $(\{Tl/Pb\}O)(SrO)$ ] with double  $[Sr(Ca,Y)Cu_2O_5]$  oxygen deficient perovskite layers, formed by sheets of corner-sharing  $CuO_5$  pyramids interleaved with calcium and/or yttrium ions as shown in Fig. 1. The structure of  $(Tl_{0.5}Pb_{0.5})(Ca_{1-x}Y_x)Sr_2Cu_2O_7$  resembles that of the 90 K superconductor  $YBa_2Cu_3O_7$ : the  $(Tl,Pb)-O$  layers replacing the  $Cu-O$  chains, Sr cations replacing Ba cations and Ca cations partially substituting for yttrium ions. The parent compound  $TlSr_2CaCu_2O_7$  is itself a metal, but exhibits no superconductivity at temperatures down to 4 K. The nominal Cu valency of this compound is 2.5+. On the basis of earlier studies of superconductivity in cuprates, one might believe that this system has an excess of hole carriers in the conducting  $CuO_2$  layers, which gives rise to a so-called "over-doping" state. Such a condition can be efficiently modified chemically by the stepwise substitution of  $Tl^{3+}$  by  $Pb^{4+}$ , by the substitution of  $Ca^{2+}$  by  $Y^{3+}$ , or, indeed, by the dual substitutions,  $Tl^{3+}/Pb^{4+}$ ,  $Ca^{2+}/Y^{3+}$ . A representation of the entire electronic structure phase diagram<sup>5</sup>) of  $(Tl_{1-y}Pb_y)Sr_2(Ca_{1-x}Y_x)Cu_2O_7$  is given in Fig. 2. Both the  $(Tl_{1-y}Pb_y)Sr_2CaCu_2O_7$  and  $TlSr_2(Ca_{1-x}Y_x)Cu_2O_7$  systems have the highest  $T_c$  ( $\sim 80$  K) for  $y \sim 0.5$  or  $x \sim 0.7$ . However, the  $(Tl_{0.5}Pb_{0.5})Sr_2(Ca_{1-x}Y_x)Cu_2O_7$  system exhibits superconductivity over the homogeneity range  $x = 0 \sim 0.5$ , with the superconducting transition temperature showing a maximum of 108 K at  $x = 0.2$ . Across the homogeneity range  $x = 0.6 \sim 1.0$ , the material also undergoes a metal - insulator transition at temperatures above  $T_c$ . It is to this part of the electronic phase diagram that we have found; we have also characterized a range physical property measurements across the entire homogeneity range  $x = 0$  to  $x = 1.0$ .

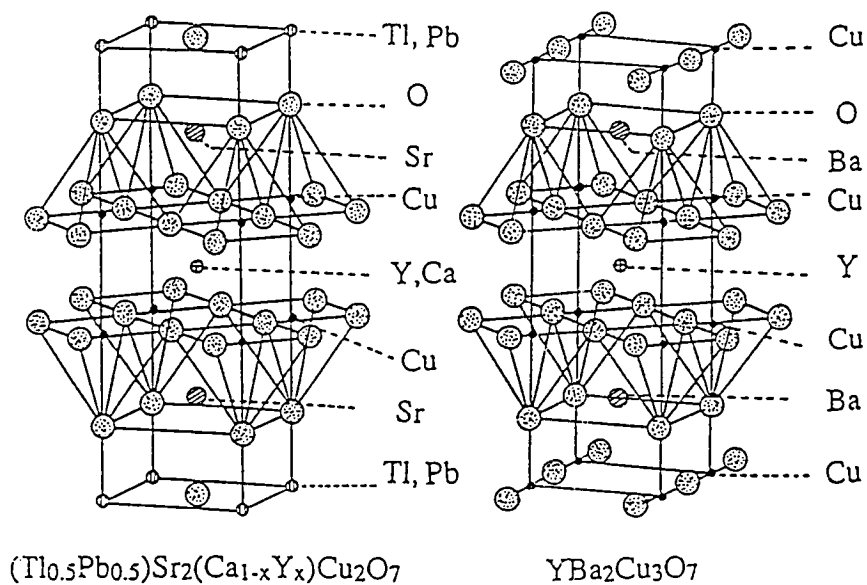


Fig. 1. A representation of the crystal structures of  $(\text{Tl}_{0.5}\text{Pb}_{0.5})\text{Sr}_2(\text{Ca}_{1-x}\text{Y}_x)\text{Cu}_2\text{O}_7$  and  $\text{YBa}_2\text{Cu}_3\text{O}_7$ .

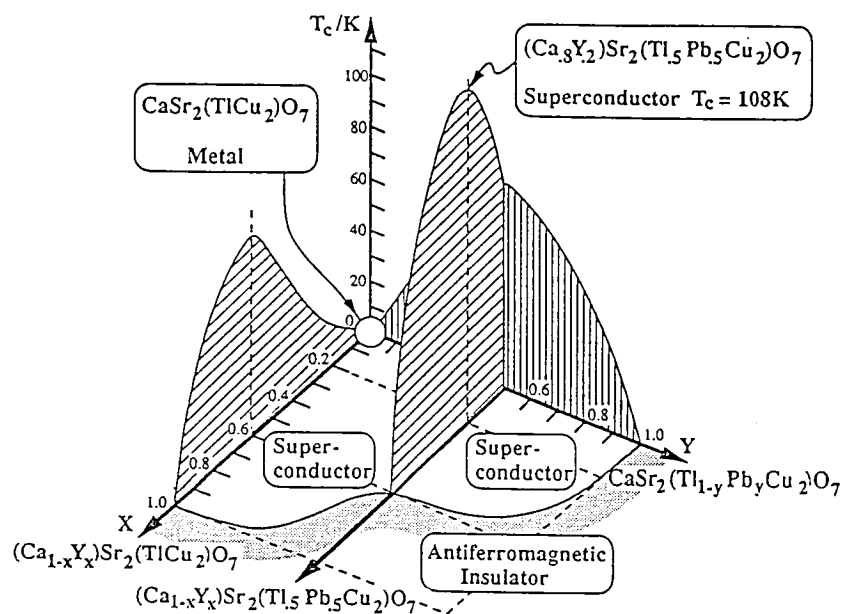


Fig. 2. Metal - Superconductor - Insulator phase diagram for the system  $(\text{Tl}_{1-y}\text{Pb}_y)\text{Sr}_2(\text{Ca}_{1-x}\text{Y}_x)\text{Cu}_2\text{O}_7$ .

## (2) Fabrication of Bi-2223 tapes and their applications in magnets and motors

Ag-clad tapes with the  $(\text{Bi,Pb})_2\text{Sr}_2\text{Ca}_2\text{Cu}_3\text{O}_{10}$  (hereafter referred to as Bi-2223) composition were prepared by the PIT (powder-in-tube) technique. Calcined powders were prepared by coprecipitation method.<sup>6)</sup> The metal nitrate salts of  $\text{Bi}(\text{NO}_3)_3 \cdot 5\text{H}_2\text{O}$ ,  $\text{Pb}(\text{NO}_3)_2$ ,  $\text{Sr}(\text{NO}_3)_2$ ,  $\text{Ca}(\text{NO}_3)_2 \cdot 4\text{H}_2\text{O}$  and  $\text{Cu}(\text{NO}_3)_2 \cdot 3\text{H}_2\text{O}$  were weighted in the mole ratio 1.7/0.4/1.8/2.2/3.2 respectively, and dissolved in ethylene glycol with nitric acid finally. The mixture of the metal nitrate solution was added to the  $\text{H}_2\text{C}_2\text{O}_4/\text{Et}_3\text{N}$  solution with virgorous stirring. During the coprecipitation process, the pH value of the solution was controlled to  $1.5 \pm 0.2$  by the addition of  $\text{Et}_3\text{N}$ . The precipitant of the pale blue powder was filtered and then dried at  $120^\circ\text{C}$ . The dehydrated powders were then calcined at  $800^\circ\text{C}$ , each particle contains Bi, Pb, Sr, Ca, Cu in appropriate ratios of cation stoichiometry. The calcined powder with the mainly  $(\text{Bi,Pb})_2\text{Sr}_2\text{CaCu}_2\text{O}_8$  (Bi-2212) phase was then packed into a silver tube, with 12 mm in outer diameter and 10 mm in inner diameter. The composite was then drawn to about 1.0-1.5 mm in outer diameter in a 15 % of area reduction per pass. Multifilamentary wires were prepared by feeding the drawn mono-core wires to a silver tube, and repeated the above drawing process. After drawing, the wire was cold rolled into a tape with thickness about 0.15 mm. The rolled tape was then sintered at  $835\text{-}840^\circ\text{C}$  for 25 - 50 h in air. After first sintering, the sintered tape was re-rolled into the thinner tape with thickness and width of 0.12 mm and 4 mm, respectively. Pancake coils were fabricated from these re-rolled tapes. Four monocore tapes were co-wound in parallel with insulation (used to separate each turn) to form a coil. Inorganic adhesive (alumina paste) was used as insulator and binder. The coil was then annealed at about  $830^\circ\text{C}$  for 50-70 h in air and slow cooled to room temperature in order to transfer the Bi-2212 phase into the Bi-2223 phase.<sup>7,8)</sup> Transport critical currents were determined by the dc four-probe technique with a criterion of  $1 \mu\text{V}/\text{cm}$ . A hall effect magnetometer (Oxford model 5200) was used to determine the central magnetic field ( $B_0$ ) generated by pancake coils at 77 K.

In Fig 3 we show a pancake coil co-wound by four 7 meter Bi-based tapes. The coil has a critical current ( $I_c$ ) of 26.3 A in the self-field and can generate a  $B_0$  of 437 G at 77 K. Prototypes of HTS pancake coil magnets have also been fabricated. Figure 4 represents a photograph of the magnet stacked by four Bi-2223 pancake coils, a  $B_0$  of 847 G at 77 K can be obtained.

Figure 5 shows a cross-sectional micrographs of Ag-sheathed 61-filamentary superconducting wires (a) intermediate stage and (b) final shape. The value of critical current density ( $J_c$ ) of this tape was  $1.3 \times 10^4 \text{ A}/\text{cm}^2$  at 77 K. In Fig. 6 we show the overview of a HTS DC motor consisted of armature (copper rotor) and magnetic field winding (HTS coil). The react-and-wind coil was fabricated by winding three 1.8 meter 19-filamentary tapes on an iron

core with diameter of 2.5 cm. The rotating speed of the fan was 1,700 rpm, as transport current was 8.7 A.

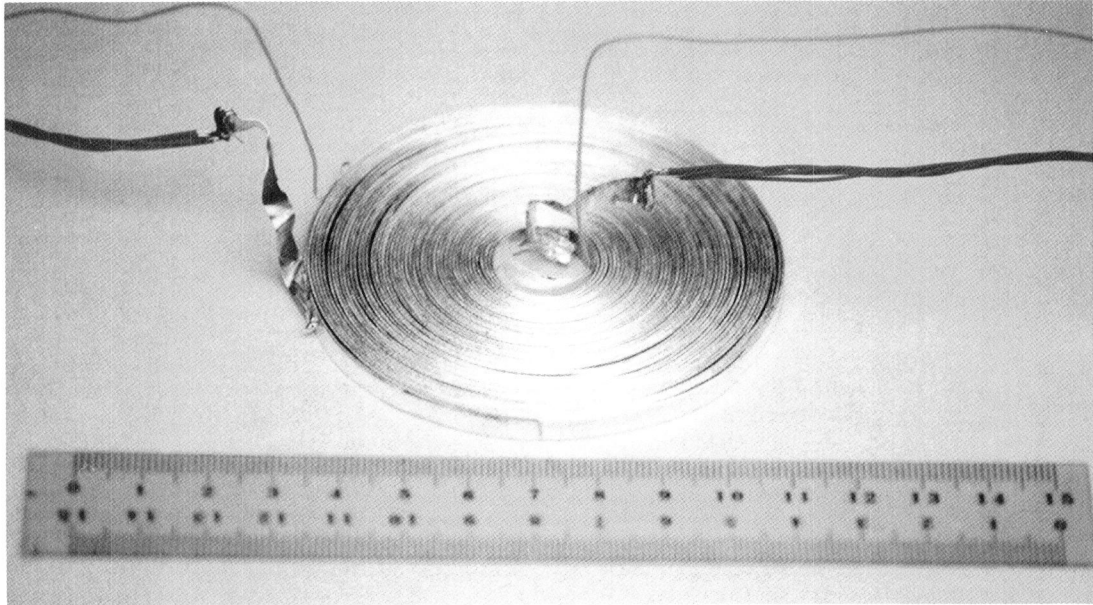


Fig. 3. A HTS pancake coil co-wound by four 7 meter Bi-based tapes, generating a center magnetic field ( $B_0$ ) of 437 G at 77 K.

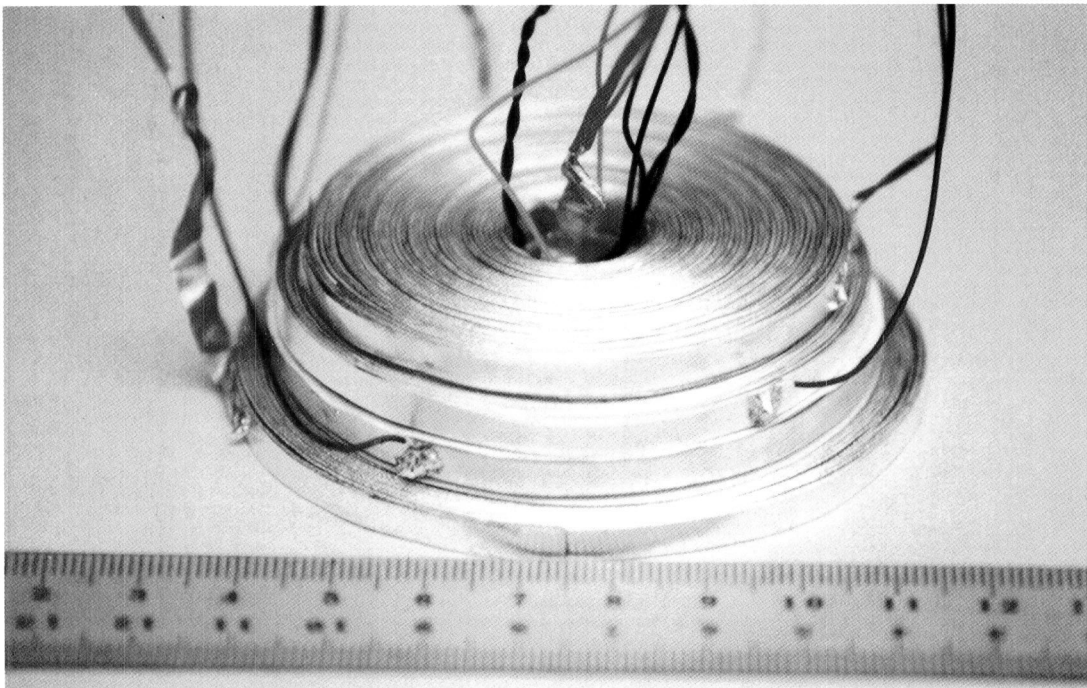


Fig. 4. A prototype of HTS magnet stacked by four pancake coils generating a center magnetic field ( $B_0$ ) of 847 G at 77 K.

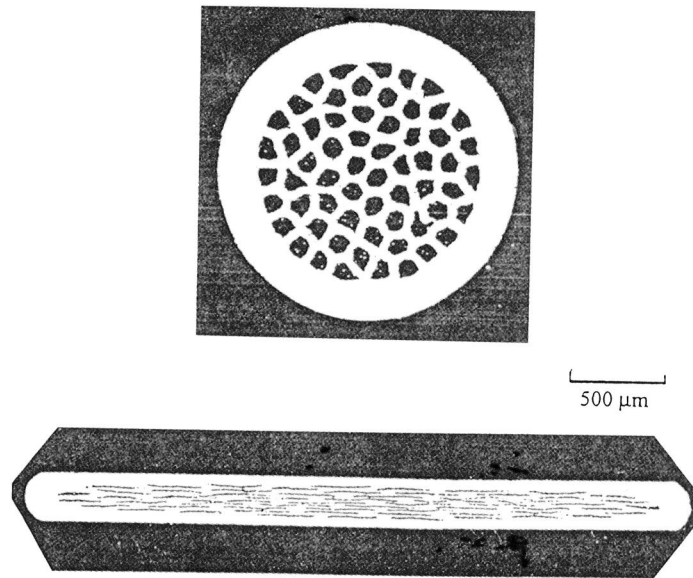


Fig. 5. Cross-sectional micrographs of Ag-sheathed 61-filamentary superconducting wires (a) intermediate stage and (b) final shape, having a  $J_c(77\text{ K}) \sim 1.3 \times 10^4$  A/cm<sup>2</sup>.

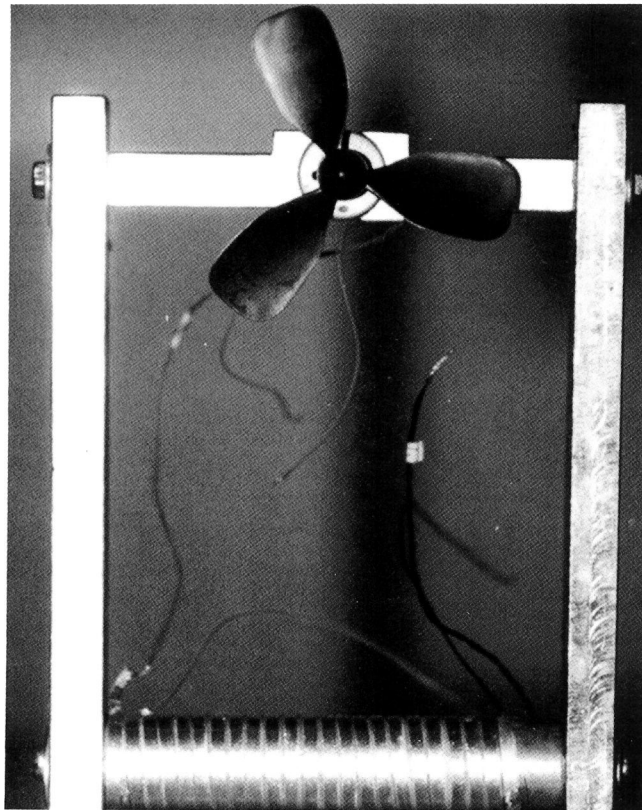


Fig. 6. A prototype of HTS DC motor prepared by winding sintered Ag-sheathed 19-filamentary tapes on an iron core to generate magnetic field, the fan speed reaching 1,700 rpm.

### (3) Fabrication of large-area Y-Ba-Cu-O Thin Films

#### (a) Hot-wall sputtering technique<sup>10)</sup>

High quality epitaxial  $\text{YBa}_2\text{Cu}_3\text{O}_{7-x}$  (YBCO) thin films have been prepared reproducibly by various deposition techniques at the MRL/ITRI. Due to the high substrate temperature and high oxidizing environment ( $P_{\text{O}_2} > 0.01$  Torr) required for in-situ growth of superconducting YBCO films, well-controlled substrate temperature is still one of the key factors in growing high quality thin films. The problem of short-life of the substrate heater has been encountered in the growing process frequently and results in the controlling difficulties of substrate temperature and uniformity of temperature on the large area substrates. Therefore, we develop a hot-wall DC sputtering deposition system, where the substrate is heated by a tube-furnace "outside" the deposition system.

The schematic picture of the hot-wall sputtering system is shown in Fig. 7. The deposition chamber was made of a quartz tube. The target was made by a solid state reaction of  $\text{Y}_2\text{O}_3$ ,  $\text{BaCO}_3$  and  $\text{CuO}$  with a stoichiometric ratio of Y:Ba:Cu=1:2:3. The sputtering gas was 50%Ar-50% $\text{O}_2$  and the total gas pressure was 1.5 torr. The gas pressure was controlled by an automatic control valve. The target-to-substrate separation was 2 cm. The sputtering current and voltage were 0.2-0.4 A and 150-200V respectively and the target dimension is 40 mm in diameter and 4 mm in thickness. The thickness of the films was 150-500 nm and deposition rate was 0.05-0.1 nm/s. After deposition, the deposition chamber was immediately back-filled with oxygen to 1 atm and the films were furnace-cooled to below 100°C in flowing oxygen.

Composition of the films grown at substrate temperatures of 750-780 °C was the same as that of the target with a stoichiometric ratio of Y:Ba:Cu=1:2:3 analysed by Rutherford Backscattering Spectroscopy (RBS). High-quality YBCO films with  $T_{c(\text{zero})}$ 's of 90 K and  $J_c(77\text{ K})$ 's in excess of  $1 \times 10^6$  A/cm<sup>2</sup> have been grown on sapphire (with a buffer layer of MgO or YSZ),  $\text{LaAlO}_3$ , MgO,  $\text{SrTiO}_3$  and YSZ substrates. The films are highly oriented with the c-axis perpendicular to the surface of the substrate.

Recently, we have scaled up the hot-wall sputtering system to grow YBCO films on two-inch substrates. The variations of the thickness and composition of the films are within 14% and 10% respectively.  $T_{c(\text{zero})}$ 's in excess of 88 K and  $J_c(77\text{ K})$ 's of  $(1.6-3.2) \times 10^6$  A/cm<sup>2</sup> can be obtained on two-inch YBCO/MgO thin films.



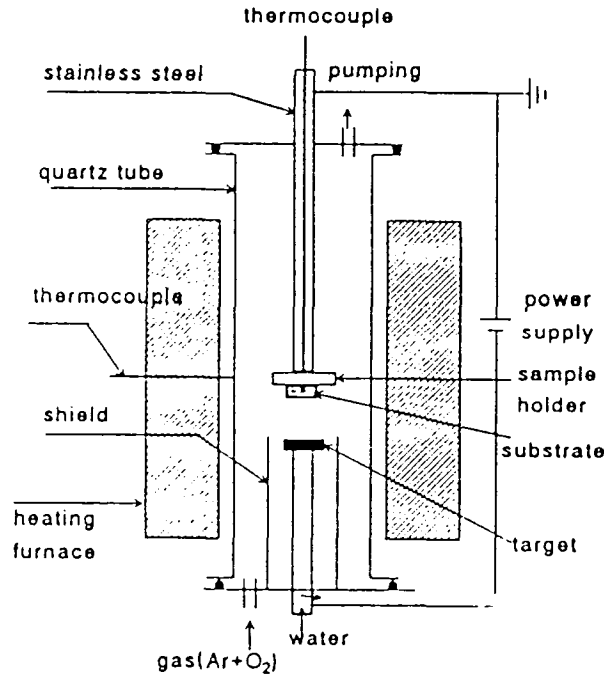


Fig. 7. Schematic picture of the hot-wall sputtering system.

#### (b) Pulsed laser ablation technique

Pulsed laser ablation (PLD) has become a widely used technique for fabricating oxide superconducting thin film due to the advantages of tolerance of high background oxygen pressures and reproducing target composition.<sup>11,12</sup> Recently, high temperature superconducting thin films have been expected to have great potential on the applications of wireless communication in the next century. Hence, the development of large-area and high quality superconducting thin films will play the most important role on producing high quality microwave devices in the future. Therefore, how to make use of the formal experiences on "small-area" for preparing high quality and "large-area" thin films by PLD is the main goal of the research.

A KrF pulsed laser system (248 nm, 25 ns and 1.5 J/cm<sup>2</sup>), as shown in Fig. 8, has been used to fabricate YBCO thin films. After carefully examining the effects of substrate temperature, laser fluence, target conditioning and target-substrate distance etc on superconducting properties, high quality Y-Ba-Cu-O superconducting thin films have been successfully prepared on (100)LaAlO<sub>3</sub> substrates. The optimal growth condition of YBCO thin films is listed as following:

Base pressure : less than  $1 \times 10^{-6}$  torr  
Substrate temperature :  $730 \text{ }^\circ\text{C}$   
Repetition rate : 5 Hz  
Laser energy density :  $1.5 \text{ J/cm}^2$   
Target-substrate distance : 4.5 cm  
 $\text{N}_2\text{O}$  gas pressure : 0.26 torr (during deposition)

$T_{c(\text{zero})}$ 's and  $J_{c(77\text{K})}$ 's in excess of 88 K and  $1 \times 10^6 \text{ A/cm}^2$  respectively can be obtained routinely.

In consideration of the uniformities of the composition and thickness in large-area, we made lots of efforts on speed of target rotation, position of laser spot and nozzle geometry design<sup>13</sup>, variation of composition and thickness within  $\pm 15\%$  in a two-inch  $\text{LaAlO}_3$  substrate have been obtained.

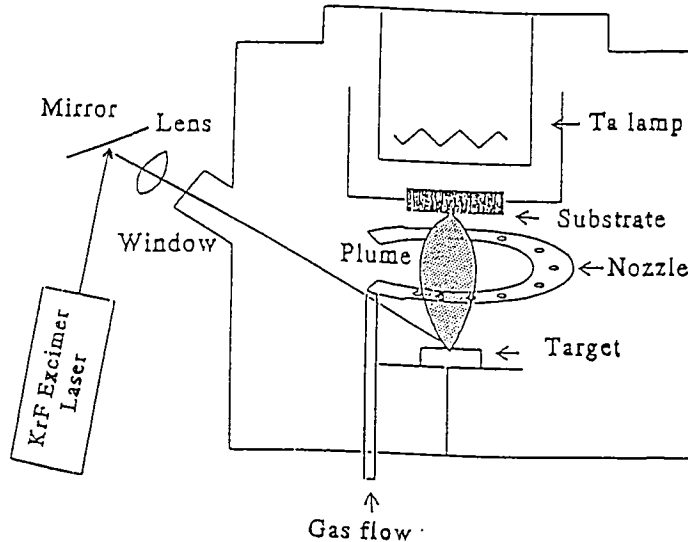


Fig. 8. Schematic picture of the laser ablation system.

#### (4) High- $T_c$ superconducting devices

##### (a) Superconducting quantum interference devices (SQUIDs)

Among the “high  $T_c$ ” weak link structures investigated, the most common are natural grain boundaries, however, they are generally randomly distributed, resulting in multiple junctions.<sup>14</sup> To avoid this problem, one of the ways for making single grain boundary

junctions, epitaxial films deposited on bicrystal substrate, has been suggested and shows some optimistic results on sensitivity and noise-reduction.<sup>15,16)</sup>

We have also successfully developed the fabrication technologies of DC-SQUIDS with highly reproducibility.<sup>17,18)</sup> The  $Tl_2Ba_2Ca_2Cu_3O_{10}$  (Tl-2223) DC-SQUIDS, patterned by standard photolithography techniques, show modulation depth (peak to peak) up to  $90\mu V$ , as shown in Fig. 9. After the successful development of the bi-epitaxial grain boundary Josephson junction at the MRL/ITRI. YBCO bi-crystal DC-SQUIDS with magnetic field modulation in excess of  $1\mu V$  can be obtained, as shown in Fig. 10.

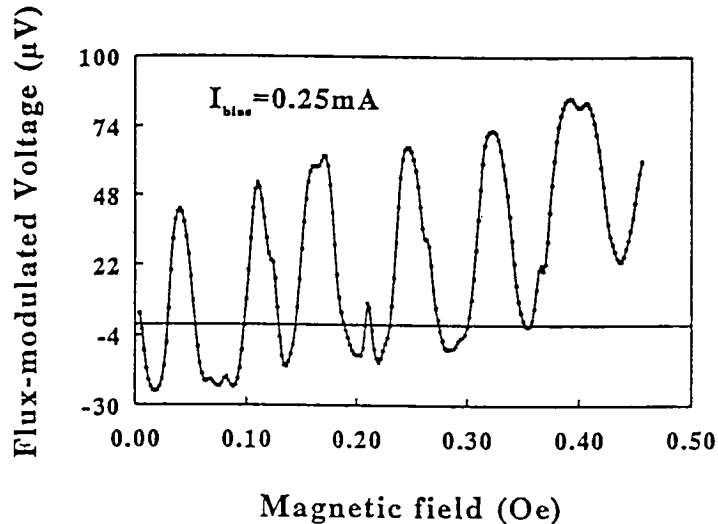


Fig. 9. Typical voltage-flux characteristic of Tl-2223 DC-SQUID at 77 K, showing the modulation depth (peak to peak) of around  $90\mu V$ .

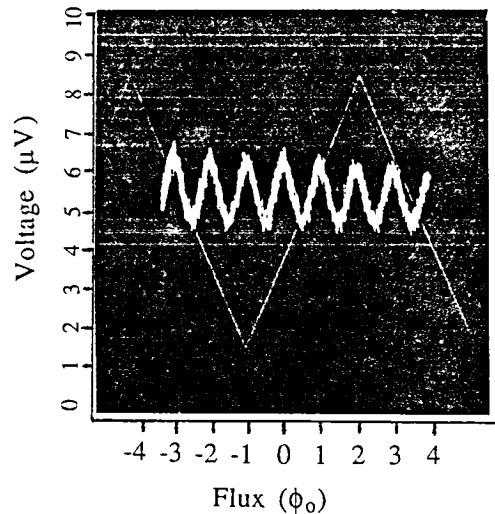


Fig. 10. A YBCO DC-SQUID prepared on (100)SrTiO<sub>3</sub> bi-crystal substrate. magnetometer at 77 K, showing the magnetic field modulation of around  $1.2\mu V$ .

(b) High- $T_c$  superconducting resonators

We have successfully fabricated and characterized coplanar 2-port transmission line resonators, suggested by Porch et al<sup>19)</sup>, using superconducting  $Tl_2Ba_2CaCu_2O_8$  thin films on (100)  $LaAlO_3$  substrates. These films were prepared by rf-sputtered Ba-Ca-Cu-O precursor films followed by Tl-diffusion technique. The resonator pattern were made by standard photolithography techniques and chemical wet etching ( $HCl : H_2O = 1 : 30$ ). The resonators were finally examined by a Wiltron 360 Network Analyzer. It was found that the unloaded quality factor ( $Q_0$ ) of linear- and meander-type resonators are larger than  $5 \times 10^3$  (5 GHz) and  $1.2 \times 10^4$  (1.6 GHz) at 77 K respectively, as shown in Fig. 11. According to the relation<sup>20)</sup> of the surface resistance ( $R_s$ ) proportional to the square of frequency ( $f^2$ ),  $R_s$  of the film at 10 GHz was estimated to be about  $800 \mu\Omega$ , which is much lower than that of  $20 m\Omega$  of commercial Au films.

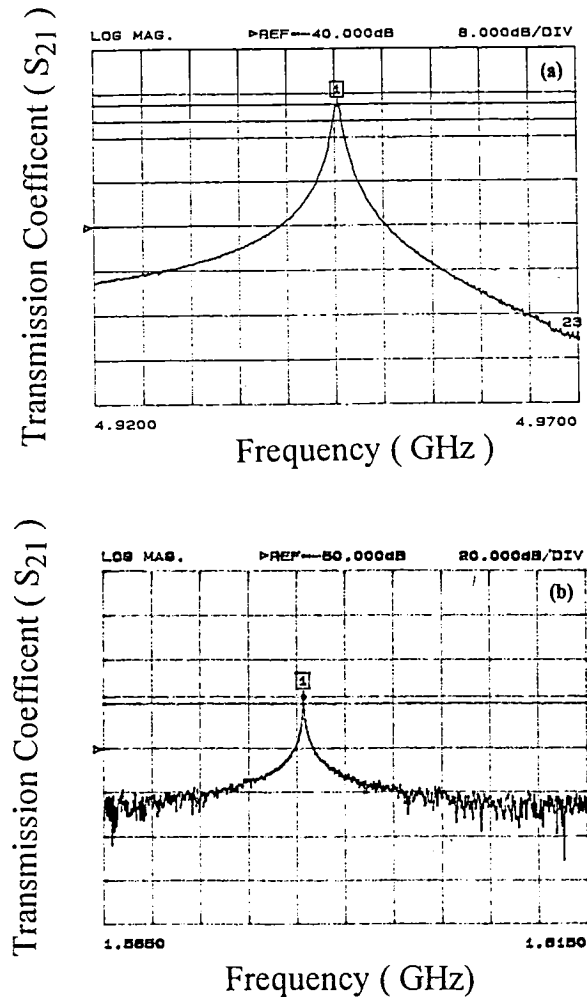


Fig. 11. Magnitude of the transmission coefficient versus frequency for (a) linear-type (b) meander-type Tl-2212 resonators.

## Acknowledgements

The authors would like to thank the Ministry of Economic affairs for the financial support of the HTS research at the MRL/ITRI. We also wish to thank Dr. H.C. Lei, Dr. K. Chen, Mr. R. J. Lin and Dr. C. J. Huang for the help to organise this manuscript.

## References

- 1) R. S. Liu, J. M. Liang, S. F. Wu, Y. T. Huang, P. T. Wu and L. J. Chen, *Physica C* **159**, 385 (1989).
- 2) P. T. Wu, R. S. Liu, J. M. Liang, Y. T. Huang, S. F. Wu and L. J. Chen, *Appl. Phys. Lett.* **54**, 2464 (1989).
- 3) J. M. Liang, R. S. Liu, Y. T. Huang, S. F. Wu, P. T. Wu and L. J. Chen, *Physica C* **165**, 347 (1990).
- 4) Y. T. Huang, R. S. Liu, W. N. Wang and P. T. Wu, *Jpn. J. Appl. Phys.* **28**, L1514 (1989).
- 5) R. S. Liu, P. P. Edwards, Y. T. Huang, S. F. Wu and P. T. Wu, *J. Solid State Chem.* **86**, 334 (1990).
- 6) D. S. Shy, W. H. Lee, and R. S. Liu, *Proceedngs of the 1994 Annual Conference of the Chinese Society for Materials Science* **1**, 290 (1994).
- 7) Y. T. Huang, S. F. Wu, and D. S. Shy, *Proceedngs of the 1994 Annual Conference of the Chinese Society for Materials Science* **1**, 332 (1994).
- 8) K. Chen, L. Horng, H. S. Koo, C. Y. Shei, L. P. Wang, C. Chiang, T. J. Yang, W. H. Lee, and P. T. Wu, *Appl. Phys. Lett.* **59**, 1635 (1991).
- 9) K. Chen, L. Hormg, C. H. Tai, J. C. Wei, T. J. Yang, and J. T. Lue, *Chinese J. Phys.* **31**, 1049 (1993).
- 10) R. J. Lin and L. J. Chen, *Appl. Phys. Lett.* **62**, 105 (1993).
- 11) D. Dijkkamp, T. Venkatesan, X. D. Wu, S.A. Shaheen, N. Jisrawi, Y. H. Min-Lee, W. L. Mclean and M. Croft, *Appl. Phys. Lett.* **51**, 619 (1987).
- 12) M. C. Foote, B. B. Jones, B. D. Hunt, J. B. Barner, R. P. Vasquez and L. J. Bajuk, *Physica C* **201**, 176 (1992).
- 13) C. M. Chang, H. C. Lai and R. J. Lin, *Proceedngs of the 1994 Annual Conference of the Chinese Society for Materials Science* **1**, 328 (1994).

- 14) B. Oh, R. H. Koch, W. J. Gallagher, V. Foglietti, G. Koren, A. Gupta, and W. Y. Lee, *Appl. Phys. Lett.* **56**, 2575 (1990).
- 15) D. Dimos, P. Chaudhari, J. Mannhart, and F. K. LeGoues, *Phys. Rev. Lett.* **61**, 219 (1988).
- 16) R. Gross, P. Chaudhari, M. Kawasaki, m. B. Ketchen, and A. Gupta, *Appl. Phys. Lett.* **57**, 727 (1990).
- 17) T. L. Chen, S. F. Wu, Y.C. Chen and R. J. Lin, *Proceedngs of the 1993 Annual Conference of the Chinese Society for Materials Science*, 7-5 (1993).
- 18) Y. C. Chen, T. L. Chen, R. J. Lin, and S. F. Wu, *Chinese Journal of Physics* **31**, 1109 (1993).
- 19) A. Porch, M. J. Lancaster, R. G. Humphreys and N. G. Chew, *Presented at Applied Superconductivity Conference, Chicago, Aug. 23-28, 1992.*
- 20) M. R. Namordi, A. Mogoro-Campero, L. G. Turner and D. W. Hogue, *IEEE Trans. Microwave Theory Tech.* **39**,1468 (1991).